

Supporting information

For ‘Cofactors involved in light-driven charge separation in photosystem I identified by sub-picosecond Infrared spectroscopy’

by Mariangela Di Donato, Andreas D. Stahl, Ivo H.M. van Stokkum, Rienk van Grondelle and Marie-Louise Groot

Experimental setup

The experimental setup (see (1, 2) for a more detailed description) for the infrared difference absorption measurements consisted of an integrated Ti:sapphire oscillator/ regenerative amplifier, operating at 1 kHz, and producing 0.8 mJ pulses of 85 fs (Hurricane, SpectraPhysics, Mountain View, CA, USA). The output of this laser was used to pump a commercial optical parametric generator and amplifier with difference frequency generation (TOPAS, Light Conversion, Vilnius, Lithuania), which resulted in a tunable output (2.5-10 μm) with a spectral width of $\sim 200\text{ cm}^{-1}$. A home-built HgCdT camera system placed behind a spectrograph was read out every shot at a repetition rate of 1 kHz and a sampling resolution between 4.5 and 6 cm^{-1} . Another part of the Hurricane output was frequency doubled in a BBO crystal to generate the pump-pulses at 700 nm ($\sim 6\text{ nm FWHM}$) with a power of 100 nJ focused to a spot of $\sim 150\text{ micrometer}$ in diameter for excitation. A moveable delay line made it possible to increase the time-of-arrival-difference of the pump-and probe beams to 3 ns. The pump beam polarization was set with a Berek-rotator (New Focus 5540, San Jose, CA, USA) to the magic angle with respect to the probe beam. A phase-locked chopper at 500 Hz ensured that every other shot the sample is excited and an absorbance difference spectrum can be calculated. To ensure a fresh spot for each laser shot, the sample was moved with a homebuilt Lissajous scanner. The setup is contained in a dry-air-purged box to reduce distortions of the infrared beam by absorption of water vapor. Homebuilt software

was used to collect data over the spectral window between 1450 and 1770 cm^{-1} in 2 partially overlapping windows. Every window was recorded with a freshly prepared sample, whose integrity was checked before and after the measurement by steady state absorption spectroscopy. At least 200 scans were averaged to obtain the final kinetic traces.

Raw data

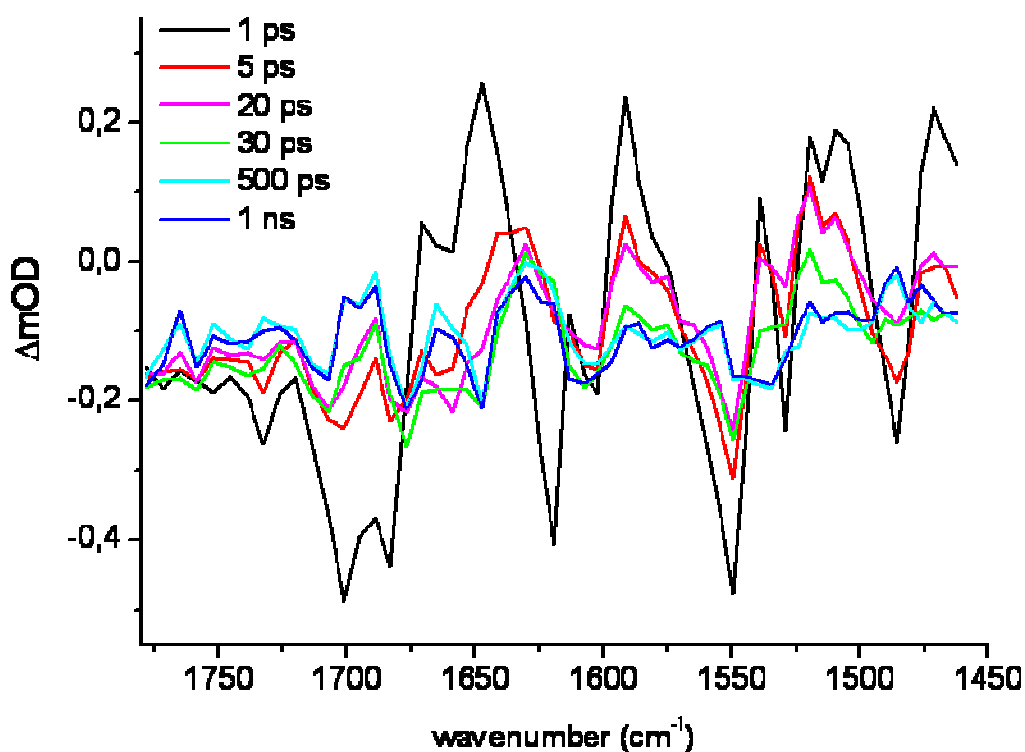


Figure S.1: Unprocessed raw data at different time delays after excitation. Wavelength calibration for the detector's channel is made by using the infrared spectrum of a polystyrene layer as reference.

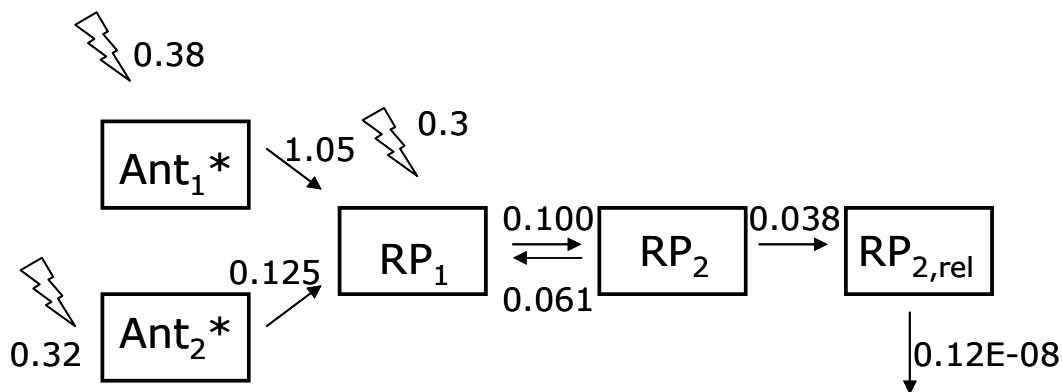
Data Analysis

Kinetic time traces were first subjected to a global fitting procedure, using a sequential scheme with increasing lifetimes. Four kinetic components with lifetimes 0.8 ps, 7.2 ± 0.7 ps, 42 ± 5 ps and a long lived component were estimated.

Target analysis-

Model 1

The first kinetic scheme applied to the data is reported in the following scheme S.1:



Scheme S.1

The kinetic scheme consists of five compartments: two excited state compartments, and three radical pair compartments, two of which are in equilibrium among each other. The SADS of the two excited state compartments are imposed to be spectrally identical, as well as those of the second and third radical pair, giving rise to only three distinct spectra for the five compartments. This spectral constraint allows the extraction of five different lifetimes, where only four resulted from the previous sequential analysis. The lifetimes resulting from our modeling well agrees with previous reports of kinetic analysis of the PSI photoinduced dynamics.(3-5)

The input excitation is distributed among the two antenna compartment and the RP_1 compartment, thus implying that upon direct excitation of the reaction center, not modeled in the scheme as a separate compartment, the RP_1 state is produced with a rate constant within our experimental time resolution. The relative excitation distribution is reported in the scheme.

In table S.1 we summarize the results of the modeling by reporting the lifetimes and the amplitude matrix for the compartments. In the amplitude matrix positive amplitudes denote decay of concentration of the corresponding compartment, and negative amplitudes rise, respectively.

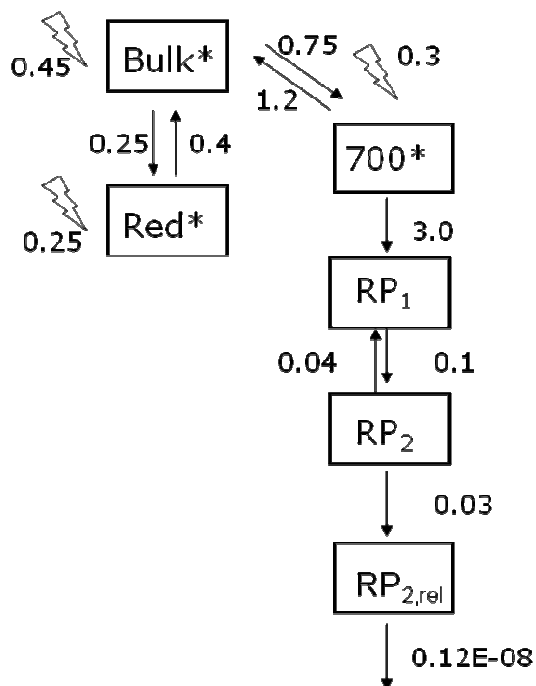
As it can be inferred from table S.1, the 0.95 ps lifetimes mainly refers to excited state decay of the antenna 1 compartment and to the appearance of the first radical pair state. The 5.6 ps lifetime mainly represents the decay of the RP_1 compartment and the rise RP_2 , while the 8 ps lifetimes has main contributions from the decay of the antenna 2 compartment and rise of RP_2 . The equilibrium between RP_1 and RP_2 decays in 46 ps with the appearance of the relaxed RP_2 form, which decays at longer times than those probed in our experiments.

Table S.1 (Model 1)

Lifetime (ps)	Ant* ₁	Ant* ₂	RP1	RP2	RP2 _{rel}
0.95	0.38	0.0	-0.42	0.045	-0.002
5.6	0.0	0.0	0.014	-0.018	0.004
8.0	0.0	0.32	0.17	-0.71	0.22
46.0	0.001	0.0	0.54	0.68	-1.22
inf	0.0	0.0	0.0	0.0	1.00

Model 2

In order to study the equilibration dynamics in the excited state, a further excited state compartment has been introduced. The target model has been thus modified as reported in scheme S.2:



Scheme S.2

In this case, the SADS of the three excited state compartments, here indicated as Bulk*, Red* and 700* are imposed to be identical. The input excitation is distributed among the two antenna compartment and the 700* compartment, which is assumed to carry 30% of the total excitation upon 700 nm irradiation. The results of the modeling are summarized in table S.2 by reporting the lifetimes and the amplitude matrix for the compartments.

Table S.2 (*Model 2*)

Lifetime (ps)	Bulk*	Red*	700*	RP1	RP2	RP2_{rel}
0.2	0.0	0.0	0.18	-0.135	0.0	0.0
1.2	0.45	-0.15	0.106	-0.45	0.06	0.0
7	0.0	0.0	0.0	0.07	-0.09	0.02
13	0.0	0.4	0.012	0.05	-0.88	0.36
50	0.0	0.0	0.0	0.46	0.9	-1.35
Inf	0.0	0.0	0.0	0.0	0.0	1.0

Finally *model 2* has been further modified by releasing the equality constrain for the Red* SADS, which allowed to extract the characteristic infrared spectrum of the red chlorophylls' pigments. The results obtained by applying *model 3* are summarized in table S.3

Table S.3 (Model 3)

Lifetime (ps)	Bulk*	Red*	700*	RP1	RP2	RP2_{rel}
0.2	-0.05	0.0	0.18	-0.13	0.0	0.0
1.2	0.38	-0.15	0.1	-0.34	0.0	0.0
7.3	0.12	0.4	0.02	-0.66	0.13	0.0
36	0.0	0.0	0.0	0.85	-2.05	1.2
70	0.0	0.0	0.0	0.28	1.91	-2.2
Inf	0.0	0.0	0.0	0.0	0.0	1.0

Interpretation of the RP1 SADS

If we accept the idea of having a different cofactor acting as a primary donor, tentative assignments can be made for the IR modes of the pigments involved in the RP1 state. The discussion is made with reference of the radical pair SADS resolved with *model 1* and reported in figure 5 in the article text.

We start with the primary acceptor A_0 , which, according to the crystal structure of PSI (6), is located in a very polar environment, having its 9-keto carbonyl H-bonded to TyrA696 and its central Mg atom unusually coordinated by MetA688 (7, 8). It is reasonable to expect that the 9-keto carbonyl absorption of A_0 will be considerably downshifted with respect to that measured in non polar solvents. Furthermore, in the anion state the carbonyl is expected to downshift even further (9). The differential signal observed at 1650(-)/1619(+) is therefore a good candidate for the 9-keto C=O of A_0 and A_0^- .

As concerns the putative primary donor, a possible candidate for its 9-keto C=O is the differential signal at 1698(-)/1711(+), since the crystal structure shows that this cofactor is not engaged in H-bonds on its carbonyl. That both P_{700} and A have no hydrogen bonds on their keto carbonyl

groups explains why the bleach at 1698 cm is constant in both RP's. The 1711 cm⁻¹ band forms a doublet with a second positive band at 1727 cm⁻¹, whereas a second possible negative feature is observed at 1689 cm⁻¹. This observation suggests the involvement of two chlorophylls. A possible explanation is the bi-directionality of the electron transfer, thus involving as primary donor both the monomer chlorophylls located on the A and B branch (ecA₂ and ecB₂ according to the nomenclature used in (8)). In this view, also two acceptor bands should be present, which is possible if the whole 1619-1595 cm⁻¹ band is attributed to the chlorophyll anion states. Another possibility is that the apparent doublet structure is the result of a combination between 9-keto and 10a-ester bands pertaining both to A and A₀.

When the spectral constraint on the red chlorophyll SADS is released, as is done in *model 3*, the spectral differences discussed earlier between RP1 and RP2 appear to be reduced. Comparing the radical pair SADS obtained by using *model 3* with those obtained with the previous two models, it is evident that, due to the role of the 'Red*' compartment at early times the RP1 SADS is in the 1630-1580 cm⁻¹ region spectrally more similar to RP2 than in *models 1 and 2*, since the 'Red*' compartment has now taken up a bit of the radical pair character of RP1.

Estimation of direct RC excitation

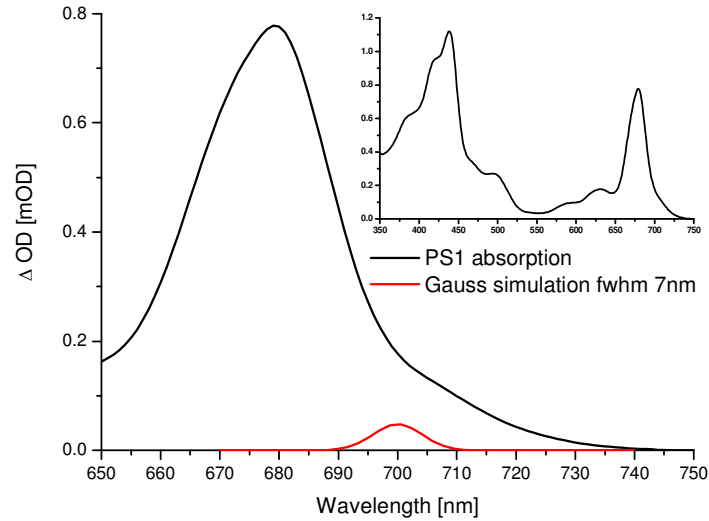


Figure S.2

Figure S.2 shows the absorption spectrum of PS1 in the Qy region (black) and a Gaussian (red) centered at 700nm with 1/50 the area and a fwhm of 7nm(10).

The Gaussian reproduces the contribution of one chlorophyll dimer to the absorption spectrum with respect to the ~100chls in the complex. This information was used to set the direct excitation of PS1RC in the target model presented in Fig 4 to 30%. The inset depicts the full range absorption spectrum of PS1 core.

Excitation at 710 and 715 nm

For experiments with red excitation, the particles were suspended in 10mM 2-(N-morpholino)ethane sulfonic acid (MES) buffer (pD 7) in D₂O containing 20mM NaCl, 20mM MgCl₂ and 0.05% β -DM. No redox mediators were added to the buffer solution, hence almost all the PSI in the sample had a closed reaction center.

The time resolved time traces obtained both with 710 and 715 nm excitation have been globally analyzed, the obtained EADS are reported in figure S.3

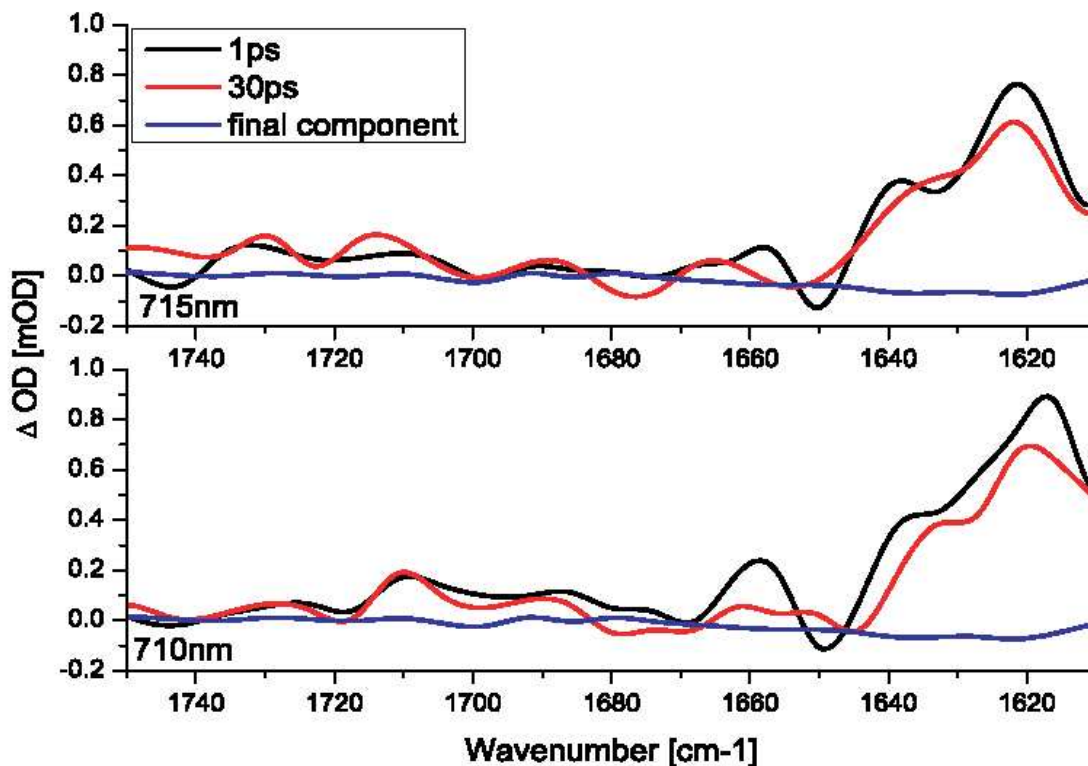


Figure S.3: EADS obtained by globally analyzing the kinetic time traces obtained upon excitation at 715 and 710 nm. Measurements have been executed on samples with closed RC, so last spectral component is flat since charge P_{700}^+ accumulation avoids the formation of the secondary radical pair $P_{700}^+A_1^-$.

In both cases the data could be fitted with three time constants of 1 ps, 30 ps and a long-lived component >2 ns plus a component that follows the instrument response function instantaneously describing the coherent interaction of the laser pulses in the sample. One of the main features in

the initial spectra is the presence of one or more bleached signals in the region between 1700 and 1650 cm^{-1} , which can be assigned to the absorption on the 13^1 keto carbonyl of one or a group of chlorophylls in the ground state. In the lower wavenumber region, roughly between 1620 and 1640 cm^{-1} , a broad positive band is present, whose specific structure differ slightly among the different experiments. This broad positive band can be ascribed to the downshifted 13^1 keto carbonyl signals in the excited state. Common to all the experiments is also the appearance of positive features in the 1710-1720 cm^{-1} region. This band is indicative of chlorophyll oxidation, since it represents the upshift of the C=O absorption upon localization of a positive charge on the pigment. The 1710 cm^{-1} band does not show significant evolution on the 30 ps timescale, except for a slight variation in intensity. The final component spectrum, which should represent the final charge separated state reached by the system, has a very small intensity in both cases. In this experiment, since no redox mediators were added to the buffer solution, in fact most of the reaction centers are closed and the initially formed radical pair decays on a ~ 30 ps time scale, since hole transfer towards P_{700} is not possible. In the small fraction of open centers, the initially formed radical pair evolves giving rise to a final charge separated state. Although the excitation power was the same as in the experiments at 700 nm excitation wavelength, namely 100 nJ, the measurements performed by exciting the sample at 710 and 715 nm are less affected by annihilation problems. This occurs because in case of far red excitation the absorption cross section of the sample is much lower (only a few chlorophylls absorb at such red wavelengths) thus the probability of having multiple excitation per center is reduced.

References

1. Groot, M.-L., van Wilderen, L. J. G. W., and DiDonato, M. (2007) Time-resolved methods in biophysics. 5. Femtosecond time-resolved and dispersed infrared spectroscopy on proteins *Photochemical & Photobiological Sciences* 6, 501-507
2. Groot, M.-L., van Wilderen, L. J. G. W., Larsen, D. S., van der Horst, M. A., van Stokkum, I. H. M., Hellingwerf, K. J., and van Grondelle, R. (2003) Initial Steps of Signal Generation in Photoactive Yellow Protein Revealed with Femtosecond Mid-Infrared Spectroscopy†, *Biochemistry* 42, 10054-10059.
3. Giera, W., Ramesh, V. M., Webber, A. N., van Stokkum, I., van Grondelle, R., and Gibasiewicz, K. (2010) Effect of the P700 pre-oxidation and point mutations near A0 on the reversibility of the primary charge separation in Photosystem I from *Chlamydomonas reinhardtii*, *Biochimica et Biophysica Acta (BBA) - Bioenergetics* 1797, 106-112.
4. Gobets, B., and van Grondelle, R. (2001) Energy transfer and trapping in photosystem I, *Biochimica et Biophysica Acta (BBA) - Bioenergetics* 1507, 80-99.
5. Holzwarth, A. R., Müller, M. G., Niklas, J., and Lubitz, W. (2006) Ultrafast Transient Absorption Studies on Photosystem I Reaction Centers from *Chlamydomonas reinhardtii*. 2: Mutations near the P700 Reaction Center Chlorophylls Provide New Insight into the Nature of the Primary Electron Donor, *Biophysical Journal* 90, 552-565.
6. Fromme, P., Jordan, P., and Krauß, N. (2001) Structure of photosystem I, *Biochimica et Biophysica Acta (BBA) - Bioenergetics* 1507, 5-31.

7. Fromme, P., and Witt, H. T. (1998) Improved isolation and crystallization of photosystem I for structural analysis, *Biochimica et Biophysica Acta (BBA) - Bioenergetics* 1365, 175-184.
8. Jordan, P., Fromme, P., Witt, H. T., Klukas, O., Saenger, W., and Krausz, N. (2001) Three-dimensional structure of cyanobacterial photosystem I at 2.5 Angstrom resolution, *Nature* 411, 909-917.
9. Mantele, W. G., Wollenweber, A. M., Navedryk, E., and Breton, J. (1988) Infrared spectroelectrochemistry of bacteriochlorophylls and bacteriopheophytins: Implications for the binding of the pigments in the reaction center from photosynthetic bacteria, *PNAS* 85, 8468-8472.
10. Küpper, H., Spiller, M., and Küpper, F. C. (2000) Photometric Method for the Quantification of Chlorophylls and Their Derivatives in Complex Mixtures: Fitting with Gauss-Peak Spectra, *Analytical Biochemistry* 286, 247-256.